Conductance in a Nanoribbon of Topologically Insulating MoS_2 in the 1T′ Phase

Viktor Sverdlov, Al-Moatasem Bellah El-Sayed, Hans Kosina, *Member, IEEE*, and Siegfried Selberherr, *Life Fellow, IEEE*

***Abstract*— The use of new materials with advanced properties has become mandatory to meet the needs for higher electronics performance at reduced power. Topological insulators (TIs) possess highly conductive topologically protected edge states which are insensitive to scattering and thus suitable for energy-efficient high-speed devices. Here, we evaluate the subband structure in a narrow nanoribbon of 1T′ molybdenum disulphide using an effective k·p Hamiltonian. Highly conductive topologically protected edge modes whose energies lie within the bulk band gap are investigated on equal footing with traditional electron and hole subbands. Due to the interaction between the edge modes at opposite sides, a small gap in their linear spectrum opens up in a narrow nanoribbon. This gap is shown to sharply increase with the perpendicular out-of-plane electric field, in contrast to the behavior in a wide nanoribbon with negligible edge modes' interaction. This increase leads to a rapid decrease in the ballistic nanoribbon conductance and current with the electric field, which can be used for designing molybdenum disulphide nanoribbon-based current switches.**

***Index Terms*— Ballistic conductance, k. p Hamiltonian, nanoribbons, subbands, topological insulators (TIs), topologically protected edge states.**

I. Introduction

THE 2-D materials yield the best electrostatic channel control and are suitable for achieving ultimately scaled field-effect transistors. However, defect levels are far too high [1] resulting in a carrier mobility which is too low for reliable devices. To boost the ON-current, an appropriate switching mechanism must be devised. Topological insulators (TIs) belong to a new class of materials characterized by highly conductive edge states that lie in the forbidden band gap of the bulk insulating material. These so-called edge states are topologically protected by time-reversal symmetry, which results in electron propagation without backscattering. A plausible option to control the current efficiently in a 2-D TI is to modulate scattering by moving the Fermi level into and out of the bulk bandgap [2]. If the Fermi level lies in the gap, the electrons propagate solely through the topologically protected edge without backscattering (ON-state). In contrast, the electrons from the edge states can scatter and backscatter strongly through the bulk states if the Fermi level moves out the bandgap and lies in the bulk conduction or valence band. The scattering suppresses the edge states' current by more than two orders of magnitude compared with the ON-state, thus paving the way to build an imperfect 2-D TI field-effect transistor [2].

Applying an electric field, E_z, orthogonal to a MoS_2 sheet in the topologically insulating 1T′ phase offers a knob to manipulate the bulk spin-orbit gap. With increasing field, the gap can be reduced, closed, and reopened again [3]. After reopening, the material becomes a normal dielectric, and topologically protected edge states are forbidden to exist. The ability to modulate the gap and its nature by applying an external electric field opens an alternative and complementary path to control the current flow with the gate voltage by efficiently eliminating the current carrying topologically protected states in the gap [4].

To enhance the ON-current carried by the edge states, it is beneficial to have many edges by stacking several, preferably narrower nanoribbons to decrease the transistor's footprint. However, it is not clear whether the gap between the bulk bands is going to close with the increasing electric field, as quantum confinement results in a wider gap. As the gap between the normal subbands does not close at any electric field, it is even less clear what is going to happen to the topologically protected edge modes and whether the electric current carried by the edge modes can be manipulated by applying a perpendicular electric field.

In this article, we evaluate the subband structure in a narrow nanoribbon of 1T′-MoS_2 TI as a function of the orthogonal electric field using an effective $\mathbf{k}\cdot\mathbf{p}$ Hamiltonian [3]. We find that a small gap in the spectrum of the edge states opens at $k_x = 0$ and we show that it increases with an applied electric field. The gap in the edge states is due to an interaction between the states located at the opposite edges of a narrow nanoribbon [5]. In contrast to a wide nanoribbon, it leads to a rapid decrease in the edge states' ballistic conductance with increasing electric field, which is promising for switching.

Manuscript received June 23, 2020; revised August 12, 2020; accepted September 8, 2020. Date of publication September 25, 2020; date of current version October 22, 2020. This work was supported in part by the Austrian Federal Ministry for Digital and Economic Affairs and in part by the National Foundation for Research, Technology and Development. The work of Al-Moatasem Bellah El-Sayed was supported in part by the by the Centre for International Cooperation & Mobility (ICM) of the Austrian Agency for International Cooperation in Education and Research (OeAD)—Atom-to-Circuit modeling technique for exploration of TI based ultralow power electronics—under Project IN 23/2018. The review of this article was arranged by Editor K. Kalna. *(Corresponding author: Viktor Sverdlov.)*

Viktor Sverdlov is with the Christian Doppler Laboratory for Nonvolatile Magnetoresistive Memory and Logic, Institute for Microelectronics, TU Wien, A-1040 Vienna, Austria (e-mail: sverdlov@iue.tuwien.ac.at).

Al-Moatasem Bellah El-Sayed, Hans Kosina, and Siegfried Selberherr are with the Institute for Microelectronics, TU Wien, A-1040 Vienna, Austria.

Color versions of one or more of the figures in this article are available online at http://ieeexplore.ieee.org.

Digital Object Identifier 10.1109/TED.2020.3023921

II. Method

A. Effective Hamiltonian

The inverted band structure of the 2-D MoS_2 in a 1T′ phase is well-described by the parabolic dispersion relations

$$E_p(k_x, k_y) = \delta - \frac{\hbar^2 k_y^2}{2m_y^p} - \frac{\hbar^2 k_x^2}{2m_x^p} \quad (1)$$

$$E_d(k_x, k_y) = -\delta + \frac{\hbar^2 k_y^2}{2m_y^d} + \frac{\hbar^2 k_x^2}{2m_x^d} \quad (2)$$

where $\mathbf{k} = (k_x, k_y)$ is the wave vector, $E_p\ (k_x, k_y)$ and $E_d(k_x, k_y)$ refer to the valence and conduction bands, respectively, and $m_{y(x)}^{d(p)}$ denote the effective masses [3]. The bands intersect at $k_y = \pm k_0$, where

$$k_0 = \sqrt{\frac{4\delta}{\hbar^2}\frac{m_y^d m_y^p}{m_y^d + m_y^p}}. \quad (3)$$

Without taking the spin–orbit interaction into account, the material is a semimetal provided that the Fermi level crosses the intersection points. The spin–orbit interaction makes the conduction and the valence bands interact with each other, which opens gaps around the intersection points at $k_y = \pm k_0$. The effective Hamiltonian $\mathbf{H}$ is written as [3] and (4), as shown at the bottom of the page.

Here, $v_{1(2)}$ are the velocities defining the strength of the spin–orbit interaction and αE_z describes the additional Rashba splitting between the bands due to the perpendicular electric field E_z [3], [4]. We use the constant values from [3] parameterized to discrete Fourier transform (DFT) calculations. Hence, the $\mathbf{k}\cdot\mathbf{p}$ Hamiltonian (4) reproduces the bulk electronic structure well. It gives a good quantitative agreement in the band gap and the inverted band gap [3]. The spin–orbit interaction described by the off-diagonal terms opens a gap at the intersection of the valence and conduction at $ky = \pm k0$ (Fig. 1, solid lines). The perpendicular electric field Ez reduces the gap at $ky = k0$, closes the gap at $E_z = E_0 = v_2\hbar k_0/\alpha$ (Fig. 1, dotted lines), and reopens it again for $E_z > E_0$ (Fig. 1, dashed lines) [3].

It is convenient to perform a canonical transformation of the Hamiltonian (4)

$$H'(\mathbf{k}) = \mathbf{C}^{-1}\mathbf{H}\mathbf{C} \quad (5)$$

by means of a unitary matrix $\mathbf{C}$.

$$\mathbf{C} = \frac{1}{\sqrt{2}}\begin{pmatrix} 0 & 1 & 0 & 1 \\ 0 & 1 & 0 & -1 \\ 1 & 0 & 1 & 0 \\ 1 & 0 & -1 & 0 \end{pmatrix}. \quad (6)$$

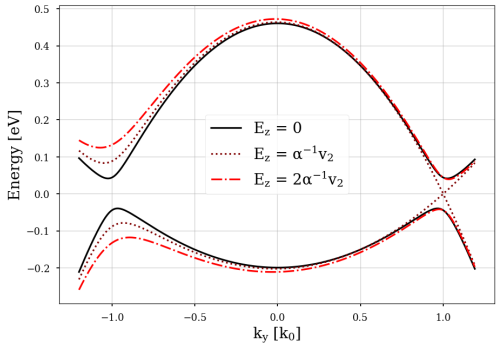

Fig. 1. Bulk energy dispersion in 1T′ z-MoS_2 2-D material, $k_x = 0$. The gaps at $k_y = k_0$ in the inverted band structure at $E_z = 0$ (solid lines) are visible. Increasing the electric field to $E_z = \alpha^{-1}v_2$ closes the gap (dotted lines) and reopens it again as a direct gap ($E_z = 2\,\alpha^{-1}v_2$, dotted-dashed lines).

After the unitary transformation, the Hamiltonian $\boldsymbol{H}'$ is in the block-diagonal form

$$\mathbf{H}' = \begin{pmatrix} H(k) & 0 \\ 0 & H^+(-k) \end{pmatrix} \quad (7)$$

where (Z^+) stands for a conjugate transpose matrix Z. The possibility to express the Hamiltonian in the form (7) is a consequence of the time-reversal symmetry.

The 2×2 Hamiltonian reads

$$H(\mathbf{k}) = \begin{pmatrix} \frac{1}{2} - k_y^2\frac{m}{m_y^p} - k_x^2\frac{m}{m_x^p} & v_2k_y - \alpha E_z + iv_1k_x \\ v_2k_y - \alpha E_z - iv_1k_x & -\frac{1}{2} + k_y^2\frac{m}{m_y^d} + k_x^2\frac{m}{m_x^d} \end{pmatrix} \quad (8)$$

where energy is in units of $E_0 = 2\,\delta$, the wave vectors $\mathbf{k} = (k_x, k_y)$ are in units of k_0, $m = ((m_y^d m_y^p)/(m_y^d + m_y^p))$, and $v_{1(2)}$ are the dimensionless velocities. The spin-down wave function $\Psi_\downarrow(k_x, y)$ of the lower 2×2 block $H(-k)$ of the Hamiltonian can be easily found from the spin-up solution for the upper block by the time-reversal transformation $\Psi_\downarrow(k_x, y) = -i\sigma_y\Psi_\uparrow(k_x, y)$ [5], where σ_y is the Pauli matrix. We therefore only focus on the 2×2 block Hamiltonian $H(\mathbf{k})$.

B. Subbands and Ballistic Conductance

Let us consider a nanoribbon with a width d along the OY axis. Only quantized energies E_n corresponding to the 1-D subbands are allowed. In addition, it is expected that at $E_z = 0$, two topologically protected highly conductive edge states localized at the opposite edges of a nanoribbon exist at an energy E within the inverted gap opened by the spin–orbit interaction at $k_y = \pm k_0$.

To find the subband energy E_n at a fixed momentum k_x along a nanoribbon, we first determine the values of the momentum $k_y = k_j$ along the quantization axis OY satisfying

$$\mathbf{H}(\mathbf{k}) = \begin{pmatrix} E_p(k_x, k_y) & 0 & -iv_1\hbar k_x & v_2\hbar k_y - \alpha E_z \\ 0 & E_p(k_x, k_y) & v_2\hbar k_y - \alpha E_z & -iv_1\hbar k_x \\ iv_1\hbar k_x & v_2\hbar k_y - \alpha E_z & E_d(k_x, k_y) & 0 \\ v_2\hbar k_y - \alpha E_z & iv_1\hbar k_x & 0 & E_d(k_x, k_y) \end{pmatrix} \quad (4)$$

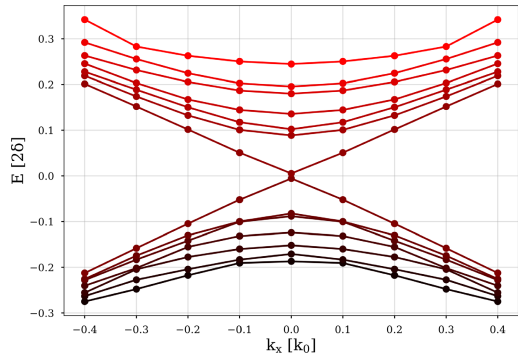

Fig. 2. Subbands in a nanoribbon of the width $d = 40/k_0$. $E_z = 0$. The subbands with almost linear dispersions corresponding to the topologically protected edge state are clearly seen.

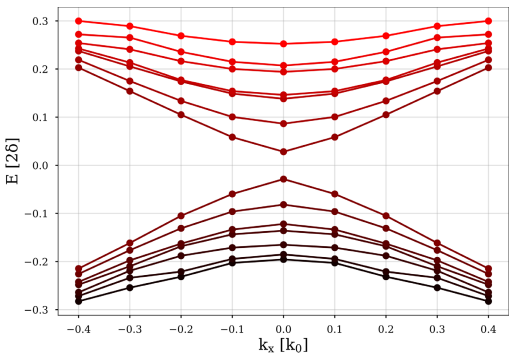

Fig. 3. Subband energies at $\alpha E_z = v_2 k_0$, when the gap at $k_y = k_0$ is closed; see Fig. 1, dotted lines.

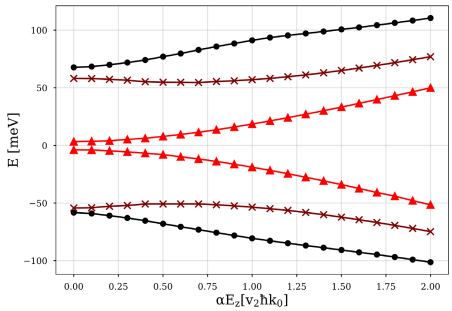

Fig. 4. Dependence of electron (hole) subband minima (maxima) on the electric field E_z for the first three subbands. In contrast to the bulk case, the gap never closes and keeps increasing with E_z.

the bulk dispersion relation in a $E_n = E(k_x, k_j)$. It can be deduced (Fig. 1) that there are four k_j,, $j = 1, \ldots, 4$, resolving the dispersion at any fixed E_n. Therefore, a general form of the subband wave function $\psi_{k_x}(y)$ in the quantization OY direction is written [6]

$$\psi_{k_x}(y) = \sum_{j=1}^{4} A_j \begin{pmatrix} 1 \\ a(k_j, E_n) \end{pmatrix} \exp(ik_j y) \tag{9}$$

where A_j are constants. Because (9) must satisfy an eigenvalue problem with the Hamiltonian (9)

$$a(k_j, E_n) = \frac{\frac{-1}{2} + k_j^2 \frac{m}{m_y^p} + k_x^2 \frac{m}{m_x^p} + E_n}{v_2 k_j - \alpha E_z + i v_1 k_x}. \tag{10}$$

The subband energies E_n are obtained by setting the wave function to zero at both the edges. The characteristic equation

$$\det(\mathbf{M}) = 0 \tag{11}$$

where the matrix $\mathbf{M} = (M_1\ M_2\ M_3\ M_4)$ is composed of the columns M_j, $j = 1, \ldots, 4$

$$M_j = \begin{pmatrix} 1 \\ a(k_j, E_n) \\ \exp(ik_j d) \\ a(k_j, E_n)\exp(ik_j d) \end{pmatrix} \tag{12}$$

is solved numerically, in complete analogy to the problem of finding the eigenenergies and eigenfunctions of a 2-band $\mathbf{k}\cdot\mathbf{p}$ Hamiltonian in silicon films [7].

The dispersions of several electron and hole subbands are shown in Fig. 2. The width d of the nanoribbon along the OY axis equals $d = 40k_0^{-1} = 28.86$ nm. The lowest electron/topmost hole subbands possess a linear dispersion. This distinguishes the subbands from traditional subbands in silicon films. The energies of these subbands lie in the bulk band gap (Fig. 1, solid lines). The subbands correspond to the topologically protected edge modes as their wave functions are localized at the edges.

A close inspection reveals that a small gap has opened at $k_x = 0$ reflecting the fact that the topological states located at the two opposite edges of the nanoribbon start interacting at $k_x \approx 0$ [5]. At larger k_x, the coupling between the edge states becomes insignificant since the edge states located at the opposite edges propagate in the opposite directions [8].

Fig. 3 shows the subbands' dispersions at an electric field of $E_z \approx v_2 \hbar k_0/\alpha$. The gap between the bulk bands would be closed at this field value in an infinitely large system (Fig. 1). However, in contrast to the bulk dispersion, the splitting between the lowest electron and topmost hole subbands in a narrow nanoribbon remains finite and actually increases compared with the case without electric field. The splitting becomes even larger at higher electric fields. As the gap between the lowest electron/topmost hole subbands grows with the electric field, their dispersion changes from linear to quadratic behavior across a broader interval of k_x.

Let us define the "bulk" gap in a nanoribbon of a finite width as the gap between the first traditional, nontopological electron, and hole subbands. Obviously, the gap does not close at $E_z = v_2 \hbar k_0/\alpha$ (Fig. 3) and keeps increasing for larger electric fields. Fig. 4 shows the dependence of the electron (hole) subband minima (maxima) $E_n^{e(h)}$ on the electric field E_z. In agreement with the dispersion relations for a 2-D sheet (Fig. 1), the "bulk" gap in a nanoribbon shows signs of a reduction with E_z (Fig. 4) until the field reaches $E_z \approx 0.7 v_2 \hbar k_0/\alpha$, after which the trend is inversed and the "bulk" gap starts increasing. This value is lower than the value $E_z < v_2 \hbar k_0/\alpha$ corresponding to the bands' inversion in the bulk (Fig. 1).

An increase in the gaps between the edge-like and traditional subbands in a nanoribbon as a function of the perpendicular electric field is reflected as a rapid decrease in the nanoribbon ballistic conductance shown in Fig. 5 (circles)

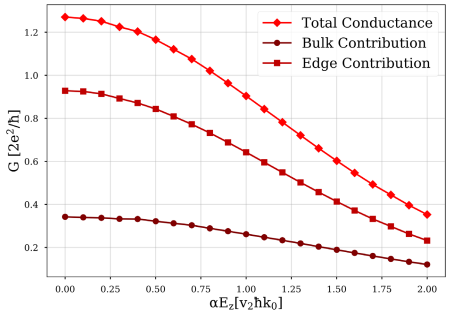

Fig. 5. Ballistic conductance (diamonds) of a 1T′ -MoS_2 nanoribbon, with the contributions from the edge states (squares) and the bulk-like subbands (circles).

computed as

$$G = \frac{2e^2}{h} \sum_i \left[\frac{1}{\exp\left\{\frac{E_i^e - E_F}{k_B T}\right\} + 1} + \frac{1}{\exp\left\{\frac{E_F - E_i^h}{k_B T}\right\} + 1} \right] \quad (13)$$

where T is the temperature and E_F is the Fermi energy. Although the edge-like subbands dominate the conductance G (Fig. 5), the two lowest (topmost) electron (hole) bulk-like contribute 30% of the ballistic conductance. However, all the contributions to the total conductance G rapidly decrease as a function of E_z (Fig. 5).

III. Discussion: Benefits and Potential Realization

The use of topologically protected edge states propagating without backscattering increases the ON-current when compared with a field-effect transistor with a 2-D channel [2], [3]. An ON-OFF ratio of two hundred is achieved by turning scattering on, if the Fermi level moves from the TI's gap into the conduction band. However, the ballistic conductance increases, when the Fermi level lies in the conduction ban as the number of transverse modes at the Fermi level is high.

Turning scattering on is achieved by changing the material from a TI to a normal dielectric without topological modes by means of an orthogonal electric field [3]. The Fermi level remains in the gap which guarantees a smaller OFF-current when compared with [2], if the bulk conductance is suppressed by scattering [4]. As the TI gap first decreases with the field, the conduction and valence bands get closer to the Fermi level, so the ballistic conductance first increases before it starts decreasing after the field-induced transition to the normal dielectric.

As the ON-current is determined by the number of topological modes, using nanoribbon devices allows making the channel narrower while maintaining the same ON-current. Alternatively, by placing several nanoribbons next to each other, one can boost the current and the current density in the ON-state when compared with a single wide nanoribbon. In addition, in a nanoribbon the gap between the bulk subbands never closes, which further decreases their contribution to transport when compared with the 2-D sample. As the gap between the edge states opens and grows, the ballistic conductance always decreases with the field, in contrast to [3] and [4]. After realistic scattering is included, we expect that the OFF-current becomes even smaller than in a wide nanoribbon. Therefore, the ON-OFF ratio from several hundred to thousand sufficient for practical applications can be achieved in a TI nanoribbon-based transistor after scattering is incorporated.

Concerning device fabrication perspectives, several nanoribbons of MoS_2 separated by a (few) monolayer(s) hBN, a 2-D wide bandgap dielectric can be vertically stacked [3] using modern assembly techniques of 2-D materials [9]. The voltage difference is applied to the top and the bottom electrodes [3]. As molecular-beam epitaxy (MBE) growth of the isolated 1T′ MoS_2 nanocrystals on a Au is now available [10], such devices could be fabricated in the near future.

IV. Conclusion

The subband structure in a narrow nanoribbon of 1T′ molybdenum disulphide as a function out-of-plane electric field was evaluated using the effective four-band $\mathbf{k}\cdot\mathbf{p}$ Hamiltonian. It is shown that by an appropriate unitary transformation, the Hamiltonian can be recast in a convenient block-diagonal form used to describe TIs. In contrast to the behavior in a wide nanoribbon where the bulk gap closes at a certain field value and becomes direct at higher values of the electric field, the gap between the traditional lowest electron and highest hole subbands never closes and increases with the perpendicular electric field. The edge modes' gap increases rapidly with the perpendicular electric field resulting in a substantial decrease in the contribution due to the edge modes in the ballistic conductance. As the total ballistic conductance decreases substantially, varying the electric field is an attractive option for designing molybdenum disulphide nanoribbon-based current switches with an improved ON-current and an enhanced ON-OFF ratio.

References

[1] Y. Y. Illarionov *et al.*, "Insulators for 2D nanoelectronics: The gap to bridge," *Nature Commun.*, vol. 11, no. 1, pp. 1–15, Dec. 2020, Art. no. 3385, doi: 10.1038/s41467-020-16640-8.

[2] W. G. Vandenberghe and M. V. Fischetti, "Imperfect two-dimensional topological insulator field-effect transistors," *Nature Commun.*, vol. 8, no. 1, pp. 1–8, Apr. 2017, doi: 10.1038/ncomms14184.

[3] X. Qian, J. Liu, L. Fu, and J. Li, "Quantum spin Hall effect in two-dimensional transition metal dichalcogenides," *Science*, vol. 346, no. 6215, pp. 1344–1347, Dec. 2014, doi: 10.1126/science.1256815.

[4] L. Liu and J. Guo, "Assessment of performance potential of MoS_2-based topological insulator field-effect transistors," *J. Appl. Phys.*, vol. 118, pp. 1–5, Sep. 2015, Art. no. 124502, doi: 10.1063/1.4930930.

[5] B. Zhou, H.-Z. Lu, R.-L. Chu, S.-Q. Shen, and Q. Niu, "Finite size effects on helical edge states in a quantum spin-Hall system," *Phys. Rev. Lett.*, vol. 101, pp. 1–4, Dec. 2008, Art. no. 246807, doi: 10.1103/PhysRevLett.101.246807.

[6] M. V. Durnev and S. A. Tarasenko, "Magnetic field effects on edge and bulk states in topological insulators based on HgTe/CdHgTe quantum wells with strong natural interface inversion asymmetry," *Phys. Rev. B, Condens. Matter*, vol. 93, no. 7, pp. 1–9, Feb. 2016, Art. no. 075434, doi: 10.1103/PhysRevB.93.075434.

[7] V. Sverdlov and S. Selberherr, "Silicon spintronics: Progress and challenges," *Phys. Rep.*, vol. 585, pp. 1–40, Jul. 2015, doi: 10.1016/j.physrep.2015.05.002.

[8] V. Sverdlov, A.-M. B. El-Sayed, H. Kosina, and S. Selberherr, "Topologically protected and conventional subbands in a 1T'-MoS_2 nanoribbon channel," in *Proc. EUROSOI-ULIS*, 2020, pp. 1–4.

[9] K. S. Novoselov, A. Mishchenko, A. Carvalho, and A. H. C. Neto, "2D materials and van der Waals heterostructures," *Science*, vol. 353, pp. 1–11, Jul. 2016, Art. no. aac9439, doi: 10.1126/science.aac9439.

[10] H. Xu *et al.*, "Observation of gap opening in 1T' phase MoS_2 nanocrystals," *Nano Lett.*, vol. 18, no. 8, pp. 5085–5090, Aug. 2018, doi: 10.1021/acs.nanolett.8b01953.